Title

Carneros Creek: Assessing restoration implications for a sinuous stream using 1-dimensional and 2-dimensional simulation models

Authors
Beagle, Julie
Marzion, Rachael
Matella, Mary

Publication Date
2008-12-15

Carneros Creek:
Assessing restoration implications for a sinuous stream using 1-dimensional and 2-dimensional simulation models

Julie Beagle, Rachael Marzion, Mary Matella
Landscape Architecture 227
December 15, 2008

Abstract

With the populations of anadromous salmonids in steep decline throughout California, many river restoration projects attempt to bring fish back to tributaries by enabling fish passage and creating spawning habitat. Carneros Creek, a tributary of the Napa River, is an incised and sinuous stream which poses a challenge for restoration planning land use management, as the watershed supports steelhead runs and valuable agricultural land. We documented the physical channel morphology of a 150 meter long reach in the Upper Carneros Creek using ground based Light Detection and Ranging (LiDAR) scans and assessed grain size using pebble counts in order to gain insight into restoration and management opportunities. These data provide a baseline geomorphic assessment for future restoration projects and allowed us to compare velocities predicted by 1-dimensional (1D) and 2-dimensional (2D) models. For the 1D model, we simulated flows by pulling out cross-sectional points from the LiDAR scans. Using a Manning's n value of 0.033 for clean, sinuous channels with some pools and riffles, we found 1D velocities at four cross-sections corresponded to 3.3 m/s, 2.3 m/s, 2.5 m/s, and 2.8 m/s with a mean velocity of 2.73 m/s. For the 2D model, we used FaSTMECH in U.S. Geological Survey's (USGS) Multi-Dimensional Surface Water Modeling System (MD_SWMS) based on LiDAR data. Our 2D velocity results decreased to an average of 0.85 m/s and ranged from 0 to 4.53 m/s based on local slope changes from the detailed channel morphology measurements. By adding grain size variable roughness to the 2D model, we saw a range of velocities from 0 to 1.98 m/s with an average of 0.65 m/s. We found that because 1D modeling of cross-sectional data using Manning's equation does not simulate flow curvature in bends, our 2D model can provide better-defined velocities than a 1D model. Because Carneros Creek is listed as a viable migration passage for steelhead, restoration managers concerned about the level of incision and the 'flashy' nature of the stream should consider how the variability in channel morphology and geomorphology models influence velocity predictions that are important drivers of habitat quality for migrating fish and juveniles.

Introduction

With the populations of anadromous salmonids in steep decline throughout California, many river restoration and management plans are currently directed at streams for which it is possible to save viable historic runs (Roni et al., 2002). The Napa River historically and currently supports the largest run of steelhead trout (anadromous rainbow trout, *Oncorhynchus mykiss*) within the San Francisco Bay Estuary (Leidy, 2005), and its tributaries support upstream rearing habitat in perennial pools. Carneros Creek, a 23-square kilometers (km^2) drainage basin, is one such tributary of the Napa River system, which has historically supported migrating, rearing and spawning steelhead trout (Figures 1 and 2) (Koehler, 2003).

The effects of human activities and intensive land management on the watershed threaten sustainable natural populations of steelhead trout. Following the Spanish conquest, land use of the Carneros watershed consisted primarily of intense grazing and ranching activity. Reports indicate that much stream incision probably occurred during this time period (Grossinger et al., 2003). During the second half of the twentieth century, development and the amount of commercial vineyards increased significantly (Table 1). Currently, the watershed includes primarily high value vineyards and residential zones along with some grazing and open space (Grossinger et al., 2003).

Carneros Creek poses a complicated challenge to successful fish migration and habitat restoration because of its incised, highly sinuous form and the valuable grape production in the region, which often extends to the top of the banks. Because the silt and loam soil profiles consist of marsh sediment deposits, this valley produces highly valuable wine grapes (NRCS *Soil survey*). Thus, management of Carneros Creek has historically been focused on maintaining current levels of grape production. When incised banks fail, land managers tend to react by hardening the banks, which increases velocities that fish must pass through to reach spawning habitat upstream.

Most stream bank and velocity measurements rely on 1-dimensional (1D) analysis of channel geometry, using traditional cross-sections and the Manning's equation to calculate mean cross-sectional velocity (Leopold and Dunne, 1978). We hypothesized that a 1D assessment would be inadequate in a stream as complex and dynamic as Carneros Creek, and posited that use of 2 dimensional (2D) modeling using 3-dimensional (3D) data would be more accurate and realistic in depicting stream morphology, flow conditions, and thus migration potential for steelhead. This enhancement of channel assessment techniques could help prioritize restoration investments system-wide.

The three goals of our study were to conduct:

1. **A detailed baseline geomorphic assessment of a representative reach using terrestrial Light Detection and Ranging (LiDAR) technology.**

   In addition to providing future restoration projects with accurate baseline topography, our data will enable stakeholders to monitor the rate of incision, potential for bank failure, aggradation or other physical changes to the channel.

2. **A comparison of 1D and 2D models.**

   Because constraints on time and budgets often determine the methods available for geomorphic assessments, we compared the results from our 1D and 2D models to analyze the advantages and disadvantages of each method. We also compared the models to determine if they produced significantly different results for Carneros Creek.

3. **Assess implications for restoration.**

   By synthesizing the flow data, the model outputs and bed and bank features, we assessed the fish migration potential through the reach under current conditions. Finally, we considered how LiDAR data sets and 2D modeling simulations could be effectively used for guiding investment in river restoration on a broader scale.

Methods

Our study site is a 150 meter long reach located in the middle alluvial section of Carneros Creek, approximately 500 meters (m) upstream of Old Sonoma Bridge (Figure 1). We selected this reach due to its relatively easy access points and because, based on visual inspection, the geomorphic features found in this section of Carneros Creek are characteristic of features commonly found elsewhere in the alluvial section of the channel.

We used the following approaches and methods to study our site:

1. **Review of historical documents** – In order to understand the evolution of the channel and the current watershed plan, we reviewed documents prepared by the San Francisco Estuary Institute (SFEI) and the Napa County Resource Conservation District (NCRCD). These documents contained information on historical land use, anthropogenic effects on the channel, fish habitat, and channel geomorphology.
2. **1-dimensional and 2-dimensional geomorphic assessment** – We constructed maps of our stream reach by filtering the LiDAR collected XYZ coordinates and creating a triangulated irregular network (TIN) layer, a vector-based data structure for storing terrain information in digital terrain modeling (Figure 3). For our 1D assessment, we created cross-sections from the LiDAR data at fifteen locations along the reach (Figure 4). For our 2-dimensional assessment, we performed continuous LiDAR scans (Mapteck I-Site 4400 model) at 10 sites within our 150 m reach and used a total station to tie in the

LiDAR images (LiDAR and total station locations shown in Figure 5). We used I-site Studio software and ArcView GIS to generate the LiDAR images of the channel and to create the cross-sections shown in Figure 6. We monumented our locations with rebar pins and flagging so that future surveys can reference our sites.

3. **Facies Map of the Creek Bed (Figure 7)** – After using the LiDAR data to make an accurate digital elevation model, we returned to our study site and mapped the patch locations of gravel, cobble, and sediment types onto our images in a continuous facies map of the reach.
4. **Pebble Counts –** We conducted pebble counts on two facies (Wolman, 1954). We randomly sampled approximately 100 stones from each facies and determined the full grain size distribution, from which we derived the median grain size (D_{50}) for each patch (Appendix 1).
5. **1D Data Analysis: Manning's Velocity Calculations –** We performed velocity calculations using 1.5 year return interval flow data, channel cross-section measurements, and our D_{50} measurement from the pebble counts. Paul Blank from Napa County Resource Conservation District provided 2001 through 2008 flow data for a station at Old Sonoma Road Bridge. This data includes stage height of the creek (in ft) and flow (in cubic feet per second or ft^3/s) at 15-minute intervals, allowing us to estimate flood frequency statistics for a 1.5 year frequency bankfull event (Table 2). We focused on 4 of the 15 cross-sections because they represented variation in stream curvature in our reach (Figure 4). We calculated velocities using Manning's equation $\upsilon = (1.49\, R^{2/3} s^{1/2})/n$ where R is the hydraulic radius, s is the slope of the channel, and n is the Manning roughness coefficient (we used 0.033) which increases with increasing roughness. This one-dimensional solution was derived from measures on the cross-section graphs of

channel hydraulic mean depth as a ratio of cross-sectional area divided by wetted perimeter (R = Area/Wetted perimeter) for locations at XS3, XS10, XS12, and XS14.

6. **2D Simulation Modeling**– We used the U.S. Geological Survey's (USGS) Multi-Dimensional Surface Water Modeling System (MD_SWMS) to examine and model our data. MD-SWMS is a pre- and post-processing application for computational models of surface-water hydraulics (McDonald et al., 2005). We imported our XYZ coordinates from the LiDAR data, built a triangulated irregular network (TIN) (Figure 3), and derived a grid for the Upper Carneros reach in order to run a 2D model (FaSTMECH Model) to predict velocity for a 1.5 year flow. We used the Manning's n value of 0.033 to set our drag coefficient in our first 2D model simulation based on constant roughness. Table 3 shows the input conditions we used for our 2D model, and further description of the model calculations can be found in McDonald et al. (2005) and the USGS MD-SWMS user guide. MD-SWMS provides the capability to integrate variable roughness based on grain size, so we digitized and geo-referenced our facies map of the reach to import it into the MD-SWMS model interface as an ancillary file. We then ran a 2-D solution for our reach by setting roughness values at nodes on our input condition grid fitted to our facies D_{50} values.

Results

Figure 8 shows a map of our stream reach created by transforming LiDAR collected XYZ coordinates into a TIN using ArcScene. By selecting LiDAR points along cross-section lines, we were also able to recreate a TIN from 15 cross-sections and a longitudinal profile of points along the stream centerline (Figure 9). The extracted dataset represents data collection with a traditional total station and cross-section survey. Figure 8 shows the interpolation of slopes based on the LiDAR derived TIN and figure 9 shows the interpolation of slopes based on the cross-sectional derived TIN.

1D Velocity Analysis

The calculated velocities using Manning's equation are summarized in Table 4. Using a Manning's n value of 0.033 for clean, sinuous channels with some pools and riffles (Mount 1995), we found velocities at XS3, XS10, XS12 and XS14 corresponded to 3.3 m/s, 2.3 m/s, 2.5 m/s, and 2.8 m/s, respectively, with a mean velocity of 2.73 m/s. If a Manning's n of 0.050 were used for sinuous, some pools and riffles, some stones and vegetation, our velocities at XS3, XS10, XS12 and XS14 corresponded to slower rates of 2.2 m/s, 1.5 m/s, 1.6 m/s, and 1.9 m/s, respectively, with a mean velocity of 1.80 m/s. Table 4 shows the velocity calculations based on the channel dimensions at these four cross-sections (Appendix 2).

2D Velocity Analysis

The Manning's n roughness coefficient can also be integrated into a 2-dimensional solution in which velocity changes across the stream width, as water depth, elevation and roughness vary along this horizontal plane. We used the U.S. Geological Survey's (USGS) Multi-Dimensional Surface Water Modeling System (MD_SWMS) to model velocities from constant roughness and variable roughness in our reach. Using a constant roughness value based on a Manning's n of 0.033, we calculated velocities shown in Figures 10 and 11. These figures also show the velocity solution for variable roughness. The constant roughness model produces the average velocity through the reach of 0.85 m/s with a minimum of 0 and maximum of 4.53 m/s. The variable roughness model shows a range of velocities from 0 to 1.98 m/s with an average of 0.65 m/s.

Discussion

1D modeling of channel cross-sectional data using Manning's equation does not simulate flow curvature in bends or eddies, so we expect our 2D model to provide better-defined velocities and bed shear stresses than 1D models. Our results show that in the sinuous, gravel-bedded Carneros Creek, much higher average velocities (2.73 m/s) are derived using the mean velocity equations than by using a 2D model. Our velocity results decreased to an average of 0.85 m/s when we integrated the local slope changes from the detailed channel morphology measurements. Our velocity further decreased to an average of 0.65 m/s when we varied grain size based on the facies map. While a 1D mean velocity is useful for a synoptic examination or baseline information for an incised channel as it takes into account channel shape, it does not address the dynamic bed profile, multiple and widely varying grain sizes, or sinuous form. A 2D model such as MD-SWMS is able to simulate uneven water-surface elevations, varying velocities, and flows in more than one direction in a cross-section. A 3D model would be even more realistic, as this would take into account changing velocities at depth through the water column, but we did not conduct such measurements in this study.

We assumed that flow responded instantaneously to local grain size. Hydraulic roughness in this mixed-grain system was approximated using our facies map and associated D_{50} values and we ran the 2D model using these differing grain sizes to adjust the bottom stresses and velocities. Lisle et al (2000) found that grain size has an effect on the magnitude of velocities. Specifically, when grain size is larger, velocities should be lower due to increased roughness, and the opposite is true for smaller grain sizes. By integrating the facies map into the simulations, we were able to more accurately depict the gradation of lateral velocities across the channel. We found a gradation of velocity complexity and an overall lowering of velocities simply by adding in variability to the roughness.

There are several limitations to our calculations and modeling and several opportunities to expand upon our results. This study could be enhanced by running different magnitudes of flow through the reach and calculating shear stress using the MD-SWMS model. If we were able to field verify water surface elevations we could have more accurately calibrated the model. At the time of this study, a large flow had not occurred and the data were unavailable. Another option is to continue our data collection and process it in a 3D model using velocities at depth in the water column. Vegetation is not considered in our model, although the capacity to perform ecosystem modeling exists within the MD-SWMS framework (McDonald et al., 2005). This alluvial reach of Carneros Creek is dominated by large bay laurel trees (*Umbellularia californica*) which have survived incision and bank failure by slumping their root wads down the vertical banks and stretching their roots up to the top of bank. Root density stabilizes the banks, and thus has a great impact on shear stress and bank stability (Micheli, 2002). Quantifying root density stabilization is another major component in the creek system and should be integrated into planning a restoration strategy for this stream.

Furthermore, Carneros Creek is listed as a viable migration passage for steelhead as the fish do not encounter large barriers between San Pablo Bay and the headwaters (Grossinger et al., 2003). Our findings of moderate velocities in the alluvial section of Carneros Creek contradict previous studies which have assumed that the alluvial section is a probable barrier to upstream adult migration and that it provides relatively low amounts of refugia for juveniles during high flow (Pearce et al, 2003). An adult salmonid can swim upstream during migration (between December and January) against an average velocity of 0.5 m/s, (Quinn, 2005). However, our simple mean velocity 1D model predicted high velocities indicating that fish might have trouble migrating upstream in the winter, and juveniles might get flushed out of the system, unable to find refugia because of the vertical bank structure. Conversely, the 2D model simulation indicated that there are migration pockets, shown in Figure 10, where fish could use the slower velocities due to boundary stresses and local topography, to migrate past what would otherwise appear to be a barrier due to high flows. Upon further investigation, when using the results of the variable roughness simulation, the increased drag coefficient and relative decrease in speed due to varying grain size create additional area of slower velocities through which adults could migrate.

The implications of our research for fisheries management and restoration are significant because they give a more realistic and complex view of a salmonid's experience in Carneros Creek. The 2D velocity model might direct restoration efforts by refining attempts to increase fish migration through the corridor. Instead of insisting on widening the channel uniformly to reduce velocities, we could use a combination of our bank slope map and the plan view of lateral velocities to identify where high velocities and steep banks might pose a threat to safe fish migration.

Conclusion

The implications of these findings for river restoration and adaptive management are multi-fold. With a stream as dynamic, flashy, and sinuous as Carneros Creek, we gain valuable insight into fish migration by using 2D modeling instead of basic 1D calculations for mean velocities. Depending on what level of precision and accuracy one requires, it may be worthwhile to work with a 2 or quasi-3D model of thousands of points. When working in a sinuous gravel-bedded stream, Manning's predictions are higher and unrealistic because they do not take into account the varied velocities of curves, local slope changes, and the varied drag coefficients of coarse and fine sediments.

When using a model that accounts for the varying velocities horizontally and continuously up and down stream throughout the reach, one would expect lower velocities. Our analysis demonstrated this expected result, and produced a more precise and accurate depiction of slope and potential bank failure using the LiDAR based channel morphology than a 4 or 15 cross-section interpolation of both bed and bank angles. Finally, as fish are able to navigate a multi-velocity stream (Facey and Grossman, 1992), restoration managers can improve their abilities to restore habitat and flow conditions by refining their analyses of velocity profiles to accurately reflect the complexity of a sinuous and incised channel form.

Acknowledgements

Paul Blank, Napa County Resource Conservation District
California Land Stewardship Institute (CLSI)
Matt Kondolf, UC Berkeley
Laurel Marcus, CLSI
Toby Minear, UC Berkeley
Sarah Richmond, UC Berkeley

References

Dunne, T. and Leopold, L., 1978. Water in Environmental Planning. W.H. Freeman and Company.

Facey, D. E. and G. D. Grossman, 1992. The relationship between water velocity, energetic costs, and microhabitat use in four North American stream fishes. Hydrobiologia. 239:1–6.

Grossinger, R., Striplen, C., Brewster, E., and McKee, L. 2003. Ecological, Geopmorphic, and Land Use History of the Carneros Creek watershed: A component of the watershed management plan for the Carneros Creek watershed, Napa County, California. A Technical Report of the Regional Watershed Program, SFEI Contribution 70. San Francisco Estuary Institute, Oakland, CA. 48pp.

Jones & Stokes (2006). Lower San Francisquito Creek Watershed Aquatic Habitat Assessment and Limiting Factors Analysis. Prepared for SCVWD.

Knighton, David. 1998. Fluvial Forms and Processes: A New Perspective. Hodder Arnold Publishing.

Koehler, J. 2003. Fish Habitat Assessment: A component of the watershed management plan for the Carneros Creek watershed, Napa County, California. Prepared for Stewardship Support and Watershed Assessment in the Napa River Watershed: A Calfed project. Napa County Resource Conservation District. Napa, CA. 36 pp.

Leidy, R.A et al. (CEMAR). Historical Status of Coho Salmon in Streams of the Urbanized San Francisco Estuary, California. California Fish and Game 91(4):219-254 2005

Lisle, Thomas, E., Jonathan M. Nelson, John Pitlick, Mary Ann Madej, and Brent L. Barkett. Variability of bed mobility in natural, gravel-bed channels and adjustments to sediment load at local and reach scales. Water Resources Research, Vol. 36, No. 12, Pages 3743-3755, December 2000

McDonald, R.R., Nelson, J.M., and Bennett, J.P., in press 2005, Multi-dimensional surface-water modeling system user's guide: U.S. Geological Survey Techniques and Methods, 6-B2, 136 p.

Micheli, E. R., Kirchner, JW. 2002. Effects of wet meadow riparian vegetation on streambank erosion 2. Measurements of vegetated bank strength and consequences for failure mechanics. Earth Surf. Process. Landforms 27, 687 – 697 (2002)

Pearce, S., O'Connor, M., McKee, L., and Jones, B. 2003. Channel Geomorphology Assessment: A component of the watershed management plan for the Carneros Creek watershed, Napa County, California. A Technical Report of the Regional Watershed Program, SFEI Contribution 67. San Francisco Estuary Institute, Oakland, CA. 57 pp.

Quinn,TP. 2005 The Behavior and Ecology of Pacific Salmon and Trout.
American Fisheries Society in association with University of Washington Press, Bethesda.

Roni, P. et al. A Review of Stream Restoration Techniques and a Hierarchical Strategy for Prioritizing Restoration in Pacific Northwest Watersheds. *North American Journal of Fisheries Management,* 22:1–20, 2002. American Fisheries Society 2002

Soil Survey Staff, Natural Resources Conservation Service (NRCS), United States Department of Agriculture. Web Soil Survey. Available online at http://websoilsurvey.nrcs.usda.gov/ accessed [12/10/08].

Wolman, M.G., 1954. A method of sampling coarse river-bed material. Transactions of the American Geophysical Union 35: 951-956.

Figure, Table, and Appendix Captions

Figure 1 – Site Location Map

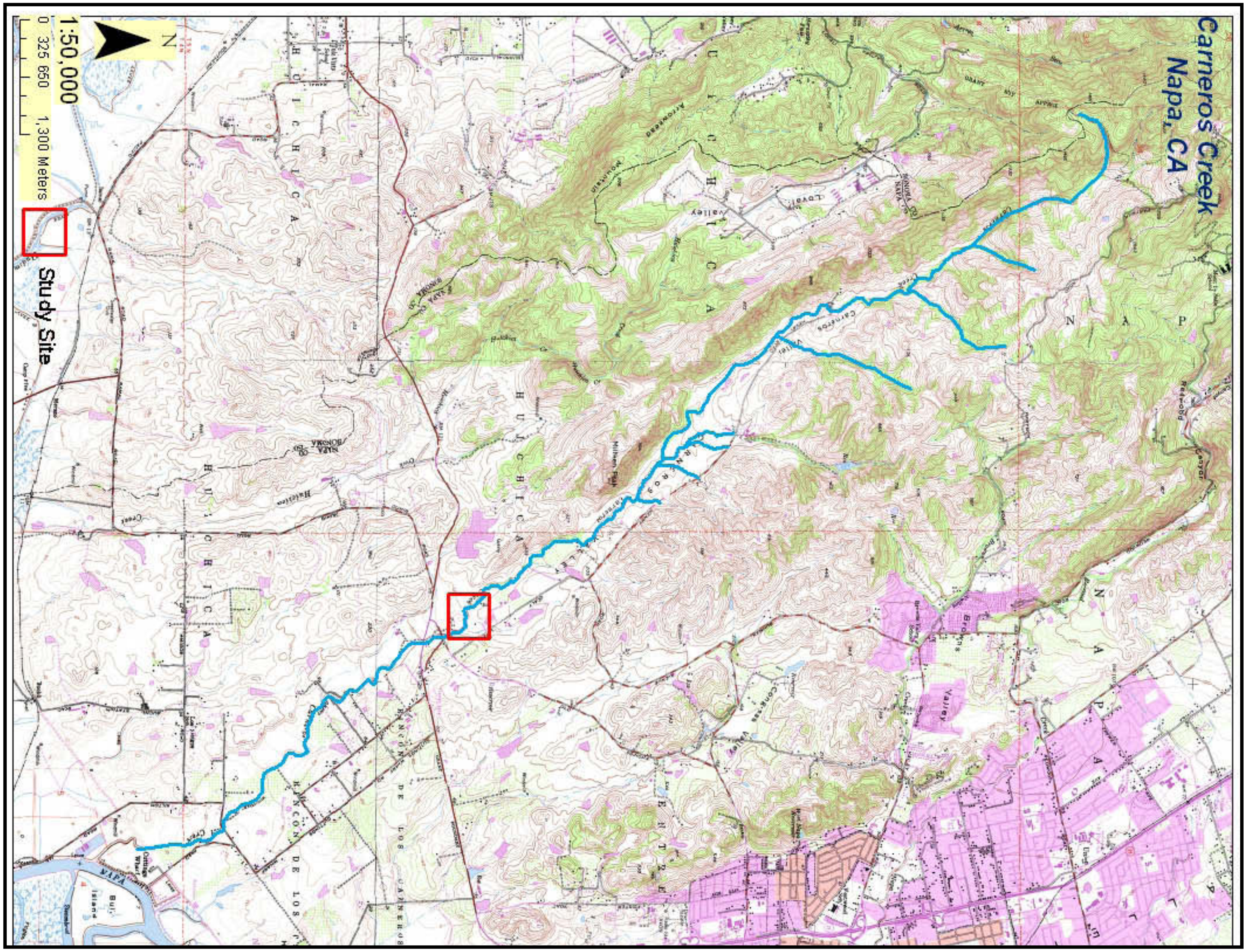

Figure 2 – Carneros Creek Watershed Map

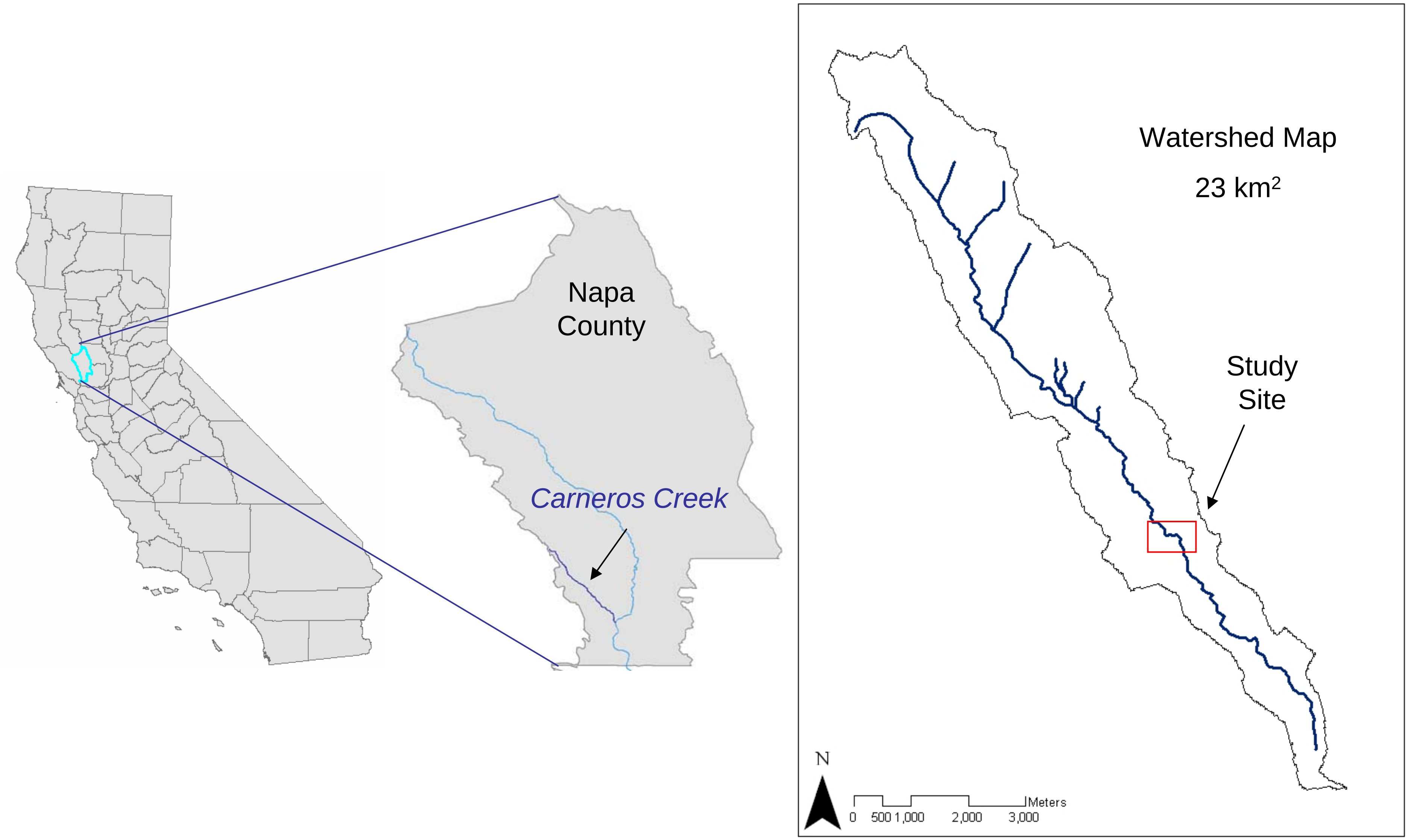

Figure 3 – Carneros Upper Reach TIN Map

Reach is located 500 meters upstream of Old Sonoma Bridge.

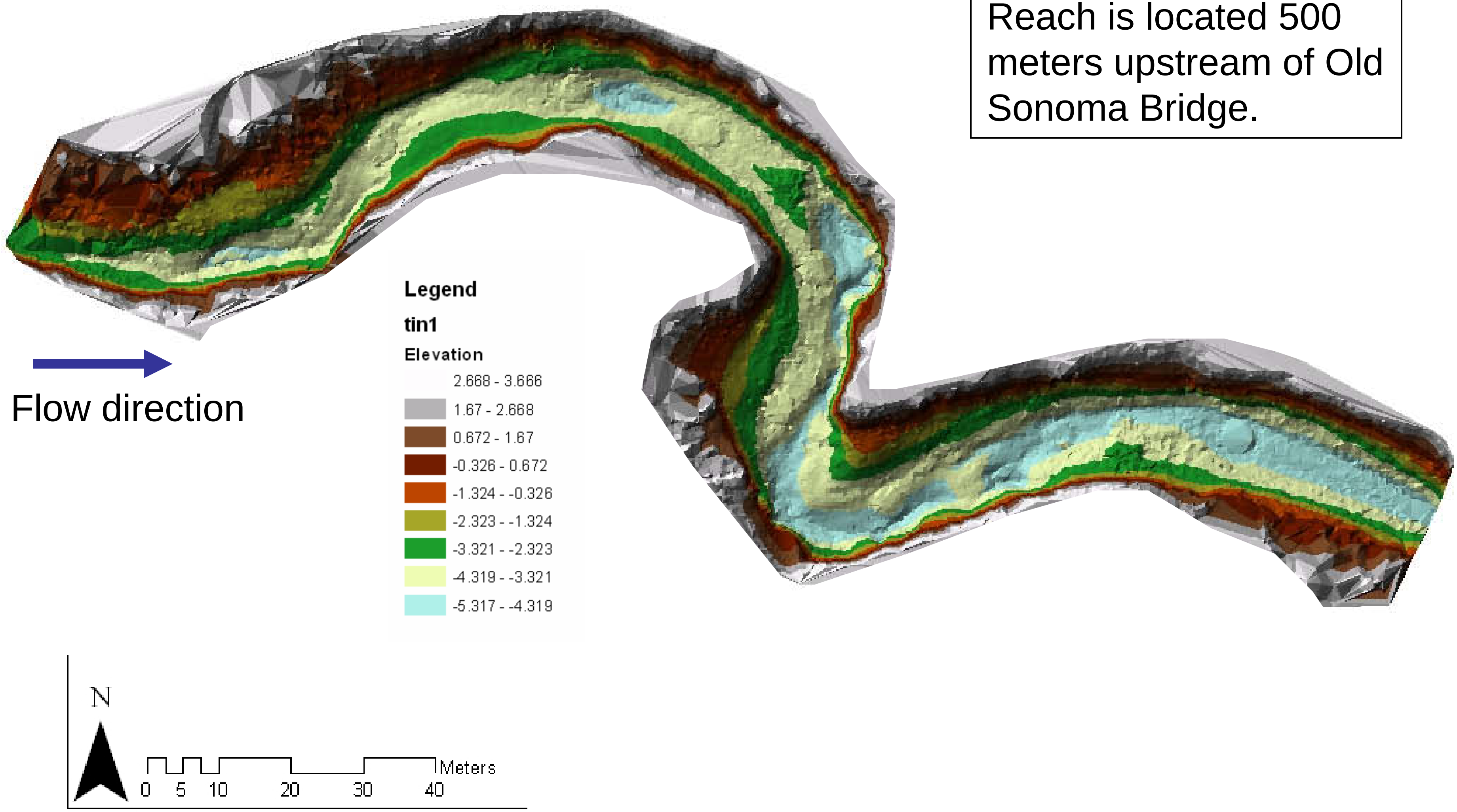

Figure 4 – Map of Cross Sections

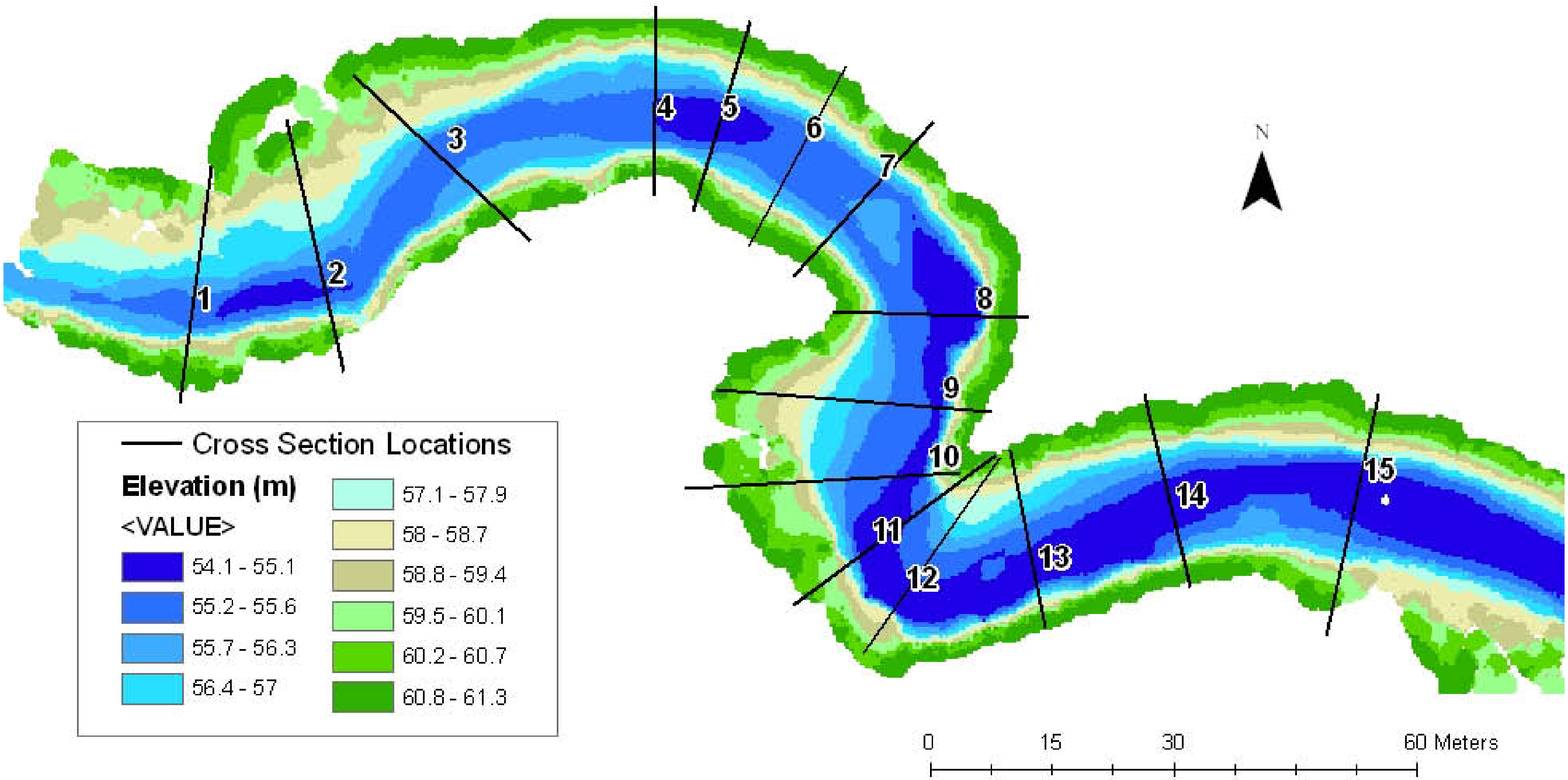

Figure 5 – LiDAR and Totals Station Locations

SITE	Description
occ1	Base station 1
occ2	Base station 2
occ3	Base station 3
li01	LiDAR Station 1
li02	LiDAR Station 2
li03	LiDAR Station 3
li04	LiDAR Station 4
li05	LiDAR Station 5
li06	LiDAR Station 6
li07	LiDAR Station 7
li08	LiDAR Station 8
li09	LiDAR Station 9
li10	LiDAR Station 10
bm1	Monument 1
bm2	Monument 2
bm3	Monument 3
Cug4 Root	Monument 4 in tree root
cug4l	Monument 4 L bank
cug4r	Monument 4 R bank
xs5LB	Monument 5
xs06RB	Monument 6
xs07	Monument 7

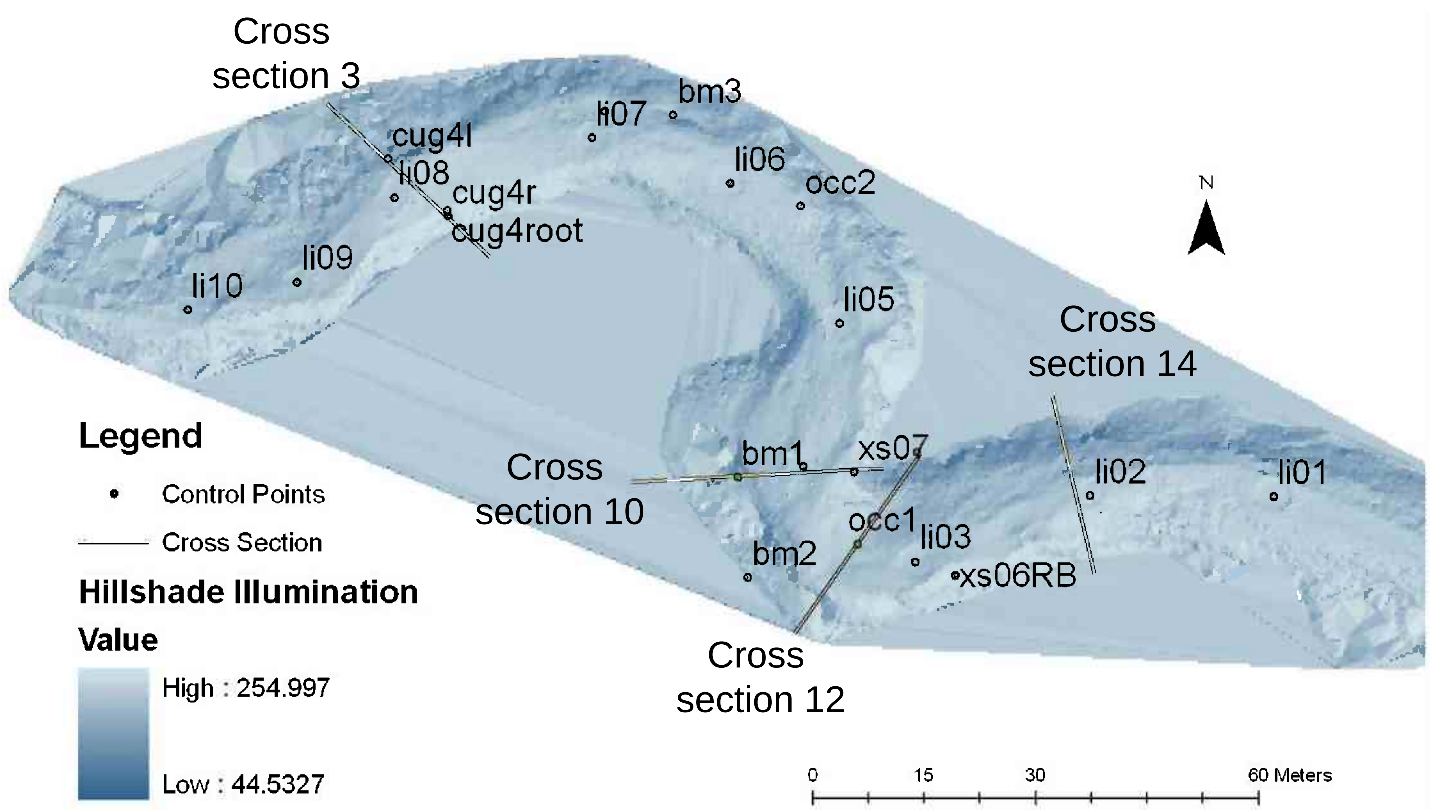

Figure 6 – Plot of Cross Sections

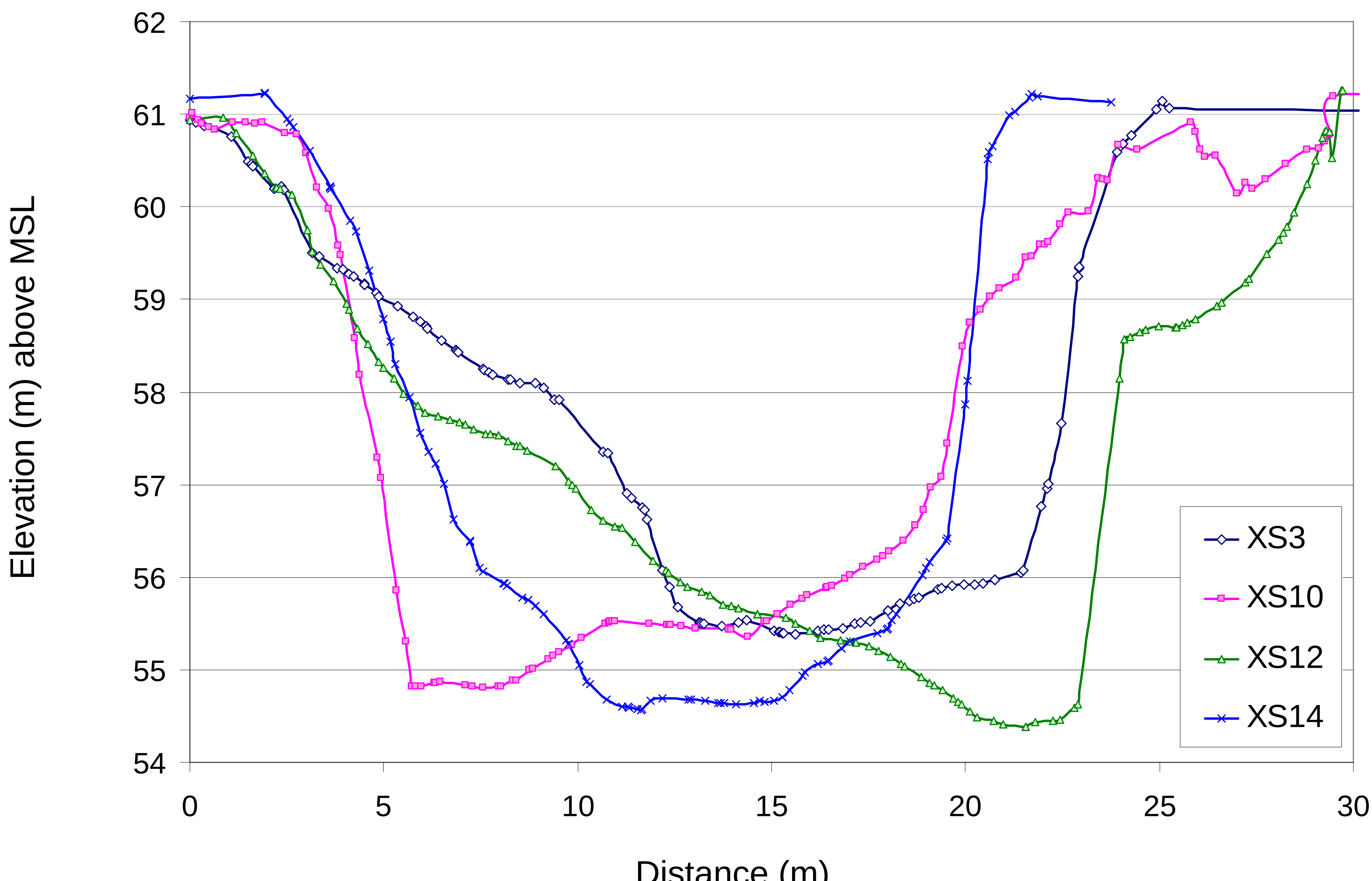

Carneros Creek looking downstream left to right bank

Figure 7 – Facies Map and Pebble Count Locations

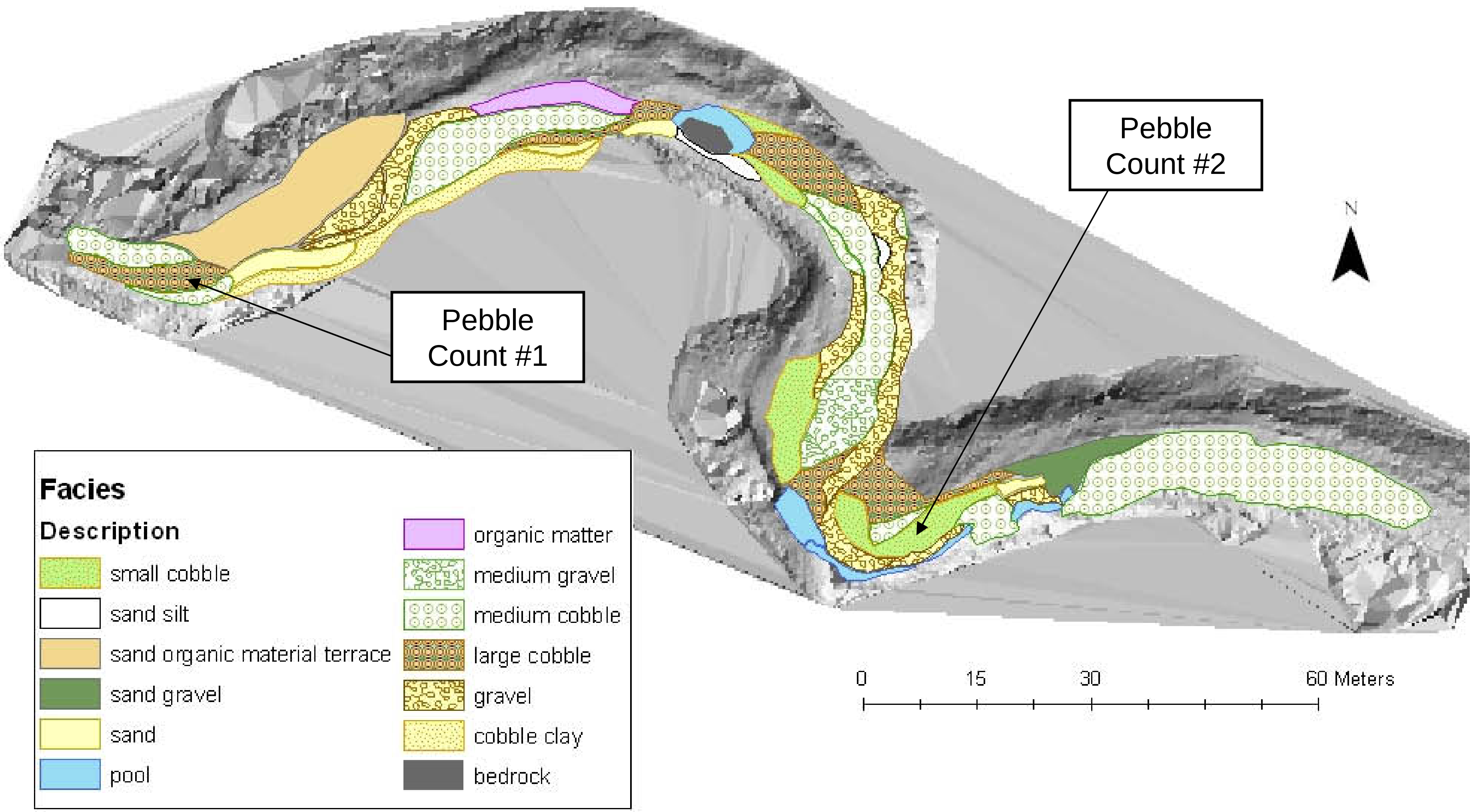

Figure 8 – Bed and Bank Slope TIN (based on LiDAR coordinates)

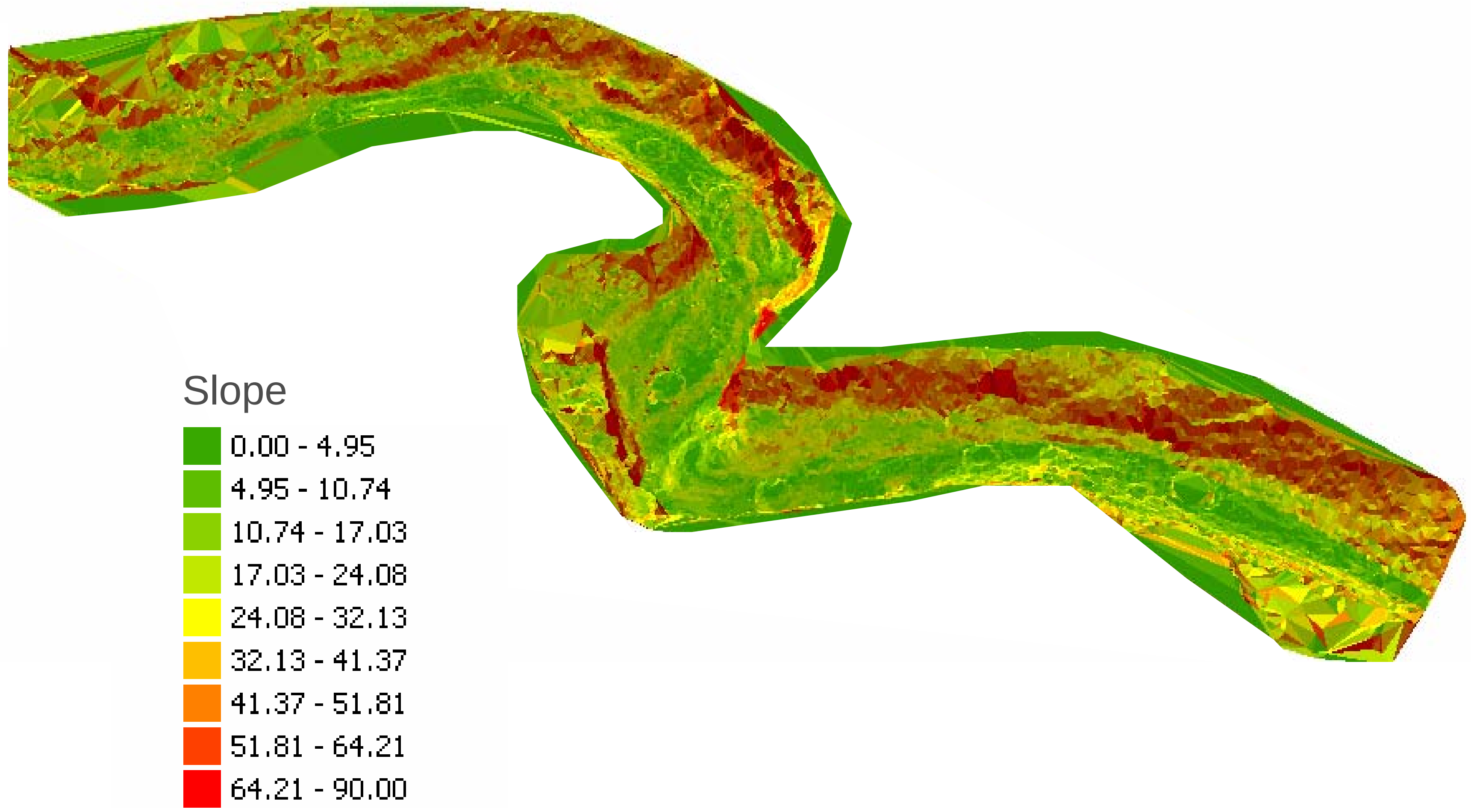

Figure 9 – Bed and Bank Slope TIN (based on cross-section points)

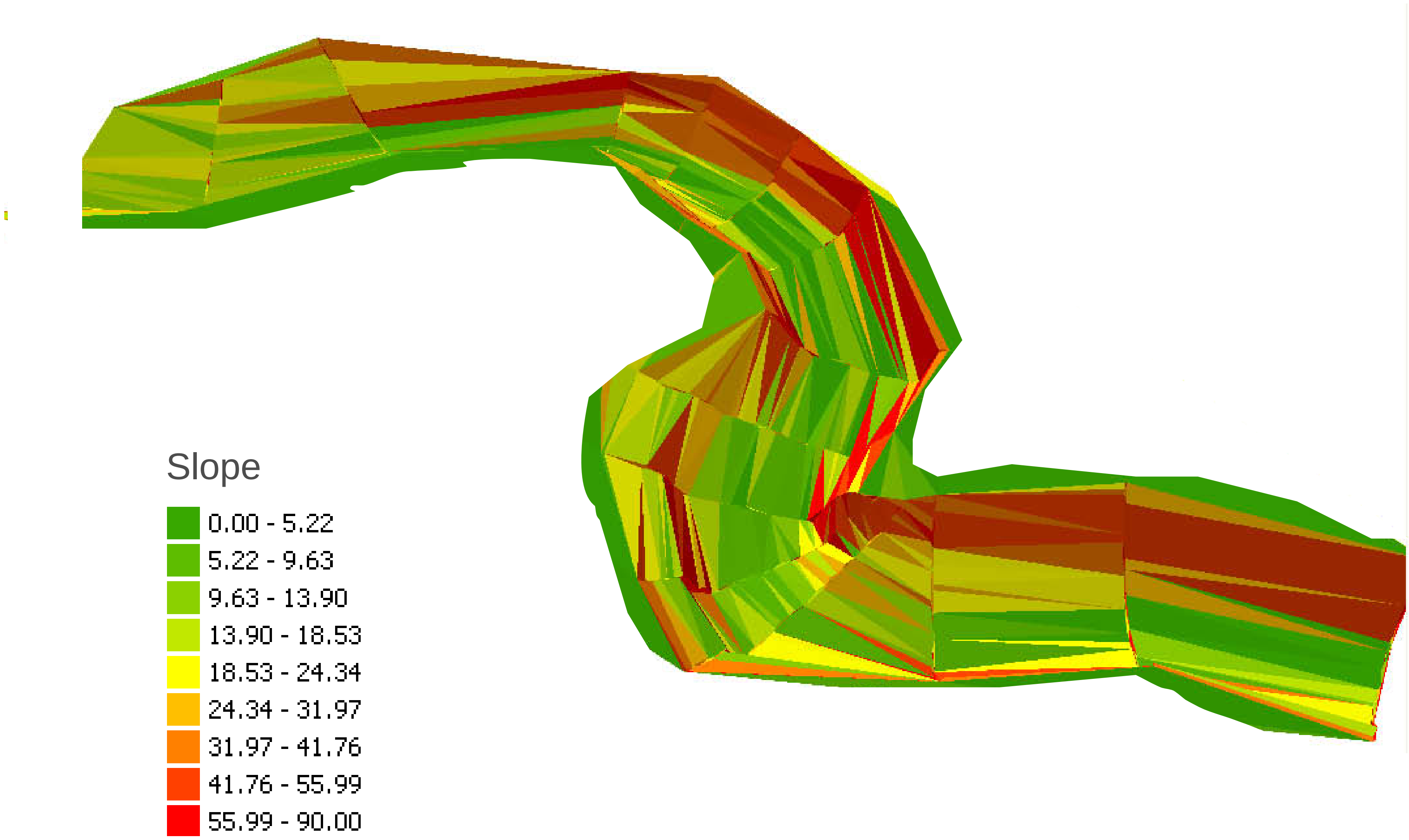

Figure 10– 2D Velocity (m/s) Solutions

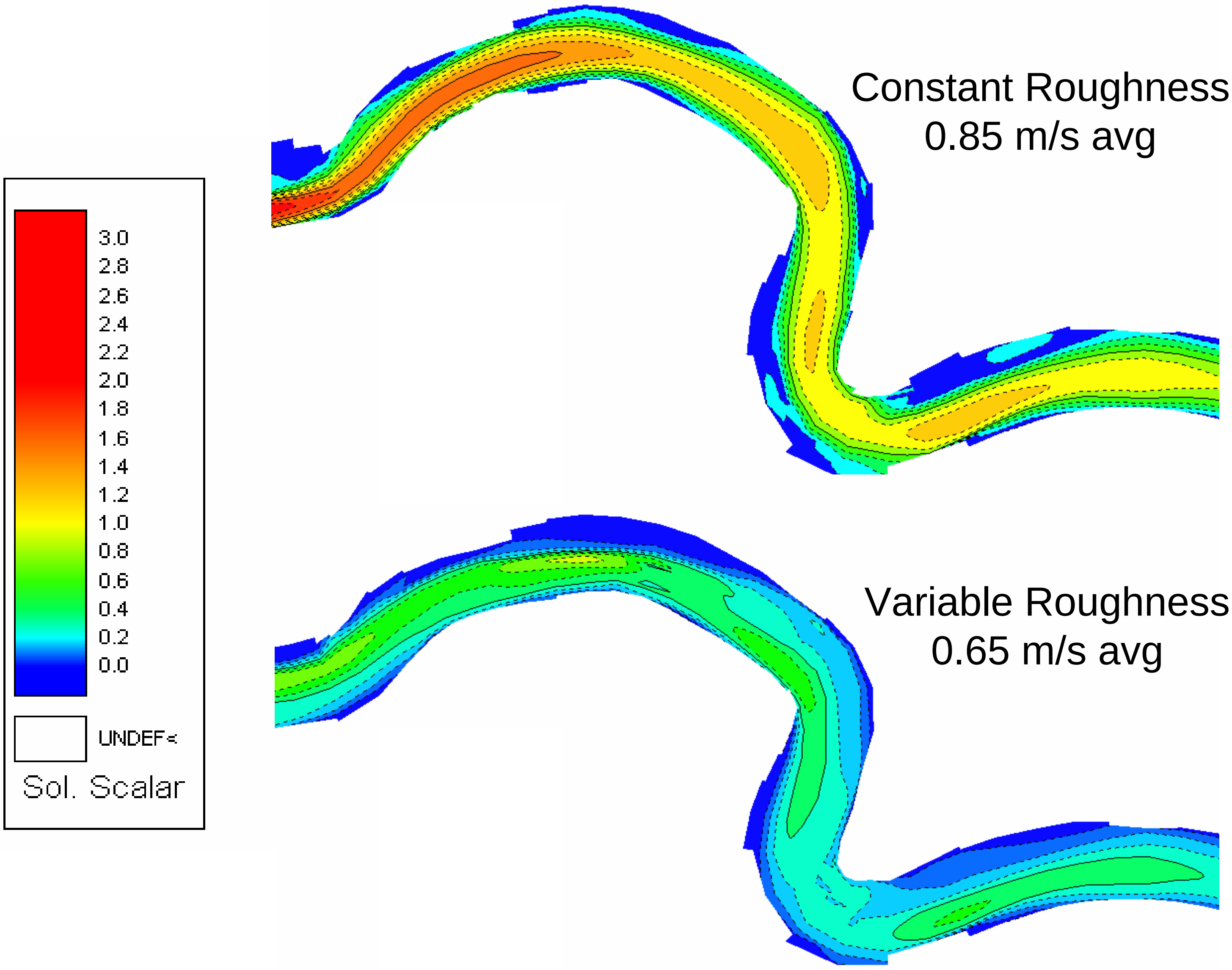

Figure 11 – 2D velocity model output in cross section form

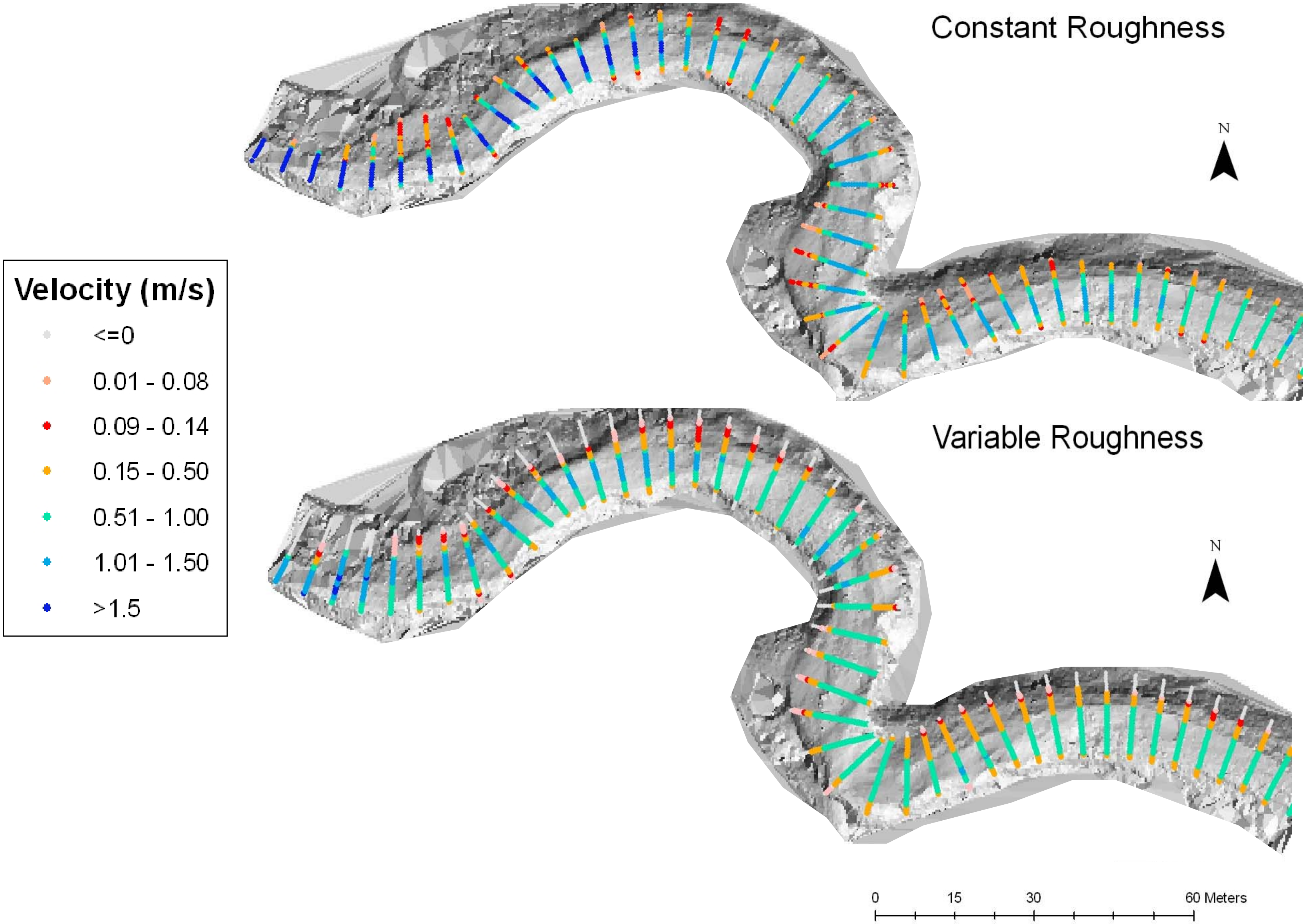

Table 1 – Land Use Table

Lower* Carneros Creek Watershed Changes 1940-1993

Land use or habitat type	ca. 1940 (acres)	1993 (acres)	% change
Developed	5	65	+1,200%
Vineyards	0	1450	--
Reservoir	0	71	--
Hay, Grain, & Misc. Ag Production	532	29	-95%
Deciduous Fruits, Nuts & Olives	449	29	-94%
Grassland/Range	1374	693	-50%
Riparian Canopy/Riverwash	88	113	+28%
Open Creek Channel	5	4	-20%
Forest, Woodland, Chaparral	76	77	+1%
Total	2,529	2,531	

Note: Based on GIS analysis of 1940/42 and 1993 aerial photography, consultation with local residents, archival references, and limited "ground-truthing."

*Below Scotts Canyon to the junction with Napa River.

Table 2 - Flood Frequency Flow Analysis

Date/Time (PST)	GH (m)	GH -e(m)	Q (m/s)	rank	RI
12/31/2005 5:45	3.54	3.44	795	1	8.00
12/16/2002 5:30	2.72	2.62	432	2	4.00
2/27/2006 20:30	1.87	1.78	242.4	3	2.67
2/25/2004 11:15	1.71	1.62	192.6	4	2.00
2/2/2008 22:15	1.42	1.36	162.6	5	1.60
12/29/2003 12:00	1.19	1.10	98.1	6	1.33
2/12/2007 19:30	0.79	0.73	46.8	7	1.14

Table 3 – Model Input Values

FaSTMECH parameters* for simulation models

	Boundary conditions		Hydraulic Properties	Initial Conditions
Model Run	**Constant discharge (cms)**	**Downstream stage constant elevation (m)**	**Drag coefficient**	**Upstream water surface elevation (m)**
1D input with constant roughness	17	57	0.0106831	NA
Water elevation height input with constant roughness	17	57	0.0106831	58
Variable roughness using D50 facies map	17	57	Variable by node	58

* Default lateral eddy viscosity, grid extension, topography, and wetting/drying parameters were used

Table 4 – Results of Manning's Equation

X-Section	U m/s (n=.033)	U m/s (n=.05)
3	3.30	2.18
10	2.34	1.55
12	2.46	1.62
14	2.82	1.86

Appendix 1 – Pebble Count Data

10/24/2008 Pebble Count 1
Julie/Sarah
Near LiDAR Scan 9
N=102
D50 = 32

Grain Size (mm)	Count	Percent	Cum Percent	Finer than (mm)
256.0	0	0.0%	100.0%	362.0
181.0	0	0.0%	100.0%	256.0
128.0	1	1.0%	100.0%	181.0
90.5	1	1.0%	99.0%	128.0
64.0	10	9.8%	98.0%	90.5
45.3	33	32.4%	88.2%	64.0
32.0	30	29.4%	55.9%	45.3
22.6	18	17.6%	26.5%	32.0
16.0	6	5.9%	8.8%	22.6
11.3	1	1.0%	2.9%	16.0
8.0	2	2.0%	2.0%	11.3
4	0	0.0%	0.0%	8.0
0	0	0.0%	0.0%	4.0
Totals	**102**	**100.0%**		

10/25/2008 Pebble Count 2
Rachael/Mary
Between LiDAR Scans 2 and 3
N=100
D50 = 16

Grain Size (mm)	Count	Percent	Cum Percent	Finer than (mm)
256.0	0	0.0%	100.0%	362.0
181.0	0	0.0%	100.0%	256.0
128.0	0	0.0%	100.0%	181.0
90.5	1	1.0%	100.0%	128.0
64.0	8	8.0%	99.0%	90.5
45.3	20	20.0%	91.0%	64.0
32.0	8	8.0%	71.0%	45.3
22.6	11	11.0%	63.0%	32.0
16.0	19	19.0%	52.0%	22.6
11.3	11	11.0%	33.0%	16.0
8.0	10	10.0%	22.0%	11.3
4	6	6.0%	12.0%	8.0
0	6	6.0%	6.0%	4.0
	100	**100.0%**		

Appendix 2. Cross-Section Profile Data (XS3, XS10, XS12, XS14)

Points	**XS3**		**XS10**		**XS12**		**XS14**	
Index	X distance (m)	Elev(m)	X distance (m)	Elev(m)	X distance (m)	Elev(m)	X distance (m)	Elev(m)
0	0	60.9333	0	60.9666	0	60.9379	0	61.171
1	0.166631	60.9175	0.056796	61.0102	0.845231	60.959	1.93112	61.22
2	0.372978	60.871	0.205561	60.9394	1.200291	60.7992	1.940127	61.226
3	1.080997	60.7537	0.299661	60.8937	1.607989	60.5502	2.499798	60.9563
4	1.489217	60.4911	0.490179	60.8596	1.916475	60.3582	2.576345	60.9098
5	1.58714	60.4585	0.65157	60.8405	2.205506	60.2124	2.653366	60.8615
6	1.625147	60.4373	1.106206	60.9161	2.2245	60.2066	3.096493	60.6083
7	2.169721	60.1986	1.452961	60.909	2.316451	60.1935	3.613915	60.2225
8	2.370926	60.2147	1.686223	60.9004	2.647702	60.1366	3.624649	60.2135
9	2.407801	60.1835	1.874002	60.9115	3.029577	59.7434	3.656197	60.1919
10	3.16641	59.5011	2.455621	60.7957	3.166676	59.5111	4.142076	59.847
11	3.333989	59.4604	2.748412	60.7831	3.359595	59.3803	4.273655	59.7319
12	3.793109	59.3413	2.991888	60.5744	3.699464	59.1949	4.636571	59.3073
13	3.939743	59.3234	3.287432	60.2084	4.027751	58.9533	4.980814	58.7905
14	4.092002	59.2772	3.581718	59.9823	4.099661	58.8873	5.166053	58.5502
15	4.233907	59.2469	3.827289	59.5853	4.318606	58.6853	5.30455	58.3016
16	4.485333	59.1653	3.894687	59.4805	4.591262	58.5243	5.654938	57.9396
17	4.495405	59.1629	4.253145	58.5825	4.869462	58.3285	5.950148	57.5579
18	4.505567	59.1584	4.390488	58.1815	4.990105	58.2637	6.163461	57.3502
19	4.802158	59.0659	4.836347	57.2929	5.260603	58.1521	6.333504	57.2264
20	4.864502	59.0291	4.91474	57.0676	5.514438	57.9745	6.538449	57.0045
21	5.354834	58.9242	5.321559	55.8565	5.869544	57.8583	6.804942	56.6184
22	5.748375	58.8076	5.577936	55.3063	6.061581	57.7809	7.215549	56.3902
23	5.941443	58.7577	5.739541	54.8242	6.392683	57.743	7.233079	56.3852
24	6.102258	58.7067	5.808606	54.8131	6.694527	57.7048	7.457529	56.0944
25	6.13563	58.6855	5.958342	54.8139	6.939811	57.6745	7.548971	56.0594
26	6.496508	58.557	6.307494	54.8567	7.094812	57.6464	8.081628	55.9344
27	6.849409	58.4498	6.350373	54.8604	7.330893	57.598	8.097667	55.9304
28	6.893311	58.4357	6.457827	54.8642	7.617958	57.5513	8.173562	55.9098
29	6.906047	58.432	7.094535	54.8275	7.758435	57.5448	8.580624	55.7826
30	6.917208	58.4286	7.272536	54.8231	7.971684	57.5355	8.738286	55.7492
31	7.553693	58.2498	7.553573	54.8064	8.198043	57.471	8.899817	55.6919
32	7.604877	58.2431	7.956489	54.8199	8.424381	57.4217	9.137495	55.5994
33	7.710881	58.2074	8.021143	54.8237	8.495884	57.4137	9.702579	55.3197
34	7.801374	58.1873	8.328575	54.885	8.696794	57.3671	9.77845	55.2762
35	8.210687	58.1374	8.412365	54.8884	9.4257	57.2049	10.03345	55.0547
36	8.27321	58.1319	8.747053	54.9946	9.777544	57.0366	10.23644	54.8765
37	8.505946	58.0957	8.857254	55.0097	9.864652	57.0001	10.31927	54.8412
38	8.894831	58.0953	9.255375	55.1141	9.943697	56.9567	10.74211	54.6733
39	9.128719	58.0415	9.38003	55.1493	10.35166	56.7315	11.15714	54.6042
40	9.400244	57.9107	9.520111	55.1925	10.64701	56.611	11.29171	54.5958
41	9.525658	57.911	9.869928	55.2727	10.96062	56.5465	11.33036	54.5951
42	10.64313	57.3511	10.11679	55.3496	11.14453	56.5307	11.53355	54.577
43	10.76234	57.3362	10.72248	55.4963	11.49068	56.3782	11.62556	54.5694
44	11.2582	56.9057	10.796	55.5137	11.9374	56.172	11.67273	54.5802

45	11.37662	56.8558	10.83226	55.5237	12.26164	56.0739	11.87728	54.6619
46	11.6683	56.7476	10.88917	55.5225	12.28201	56.0677	12.18938	54.695
47	11.70968	56.7259	10.94649	55.5212	12.33196	56.0515	12.84416	54.6824
48	11.79174	56.6228	11.84515	55.5019	12.65434	55.9449	12.90468	54.676
49	12.17295	56.0681	12.29111	55.4912	12.81775	55.8992	13.28911	54.6623
50	12.3752	55.8884	12.37098	55.4892	13.19425	55.8418	13.62786	54.6407
51	12.5853	55.6715	12.39651	55.4886	13.40908	55.8081	13.67896	54.6372
52	13.12845	55.5147	12.67636	55.473	13.758	55.7085	13.77499	54.6447
53	13.1653	55.5073	13.04938	55.4462	13.97445	55.6885	14.09172	54.6218
54	13.19226	55.5029	13.89198	55.4416	14.14012	55.6655	14.53192	54.6407
55	13.25897	55.5001	13.90765	55.4297	14.62293	55.6032	14.70049	54.6595
56	13.71108	55.4717	13.96757	55.438	14.6363	55.6015	14.82972	54.6546
57	14.15796	55.5093	14.38243	55.3569	14.64779	55.6011	15.07105	54.67
58	14.36499	55.537	14.82871	55.5196	15.37053	55.5661	15.28587	54.7071
59	15.06071	55.4264	14.87891	55.5279	15.61288	55.5024	15.46763	54.78
60	15.19444	55.4093	15.1479	55.5968	15.97586	55.4229	15.79085	54.9355
61	15.22888	55.4074	15.49707	55.6994	16.25367	55.3448	15.8512	54.9664
62	15.28847	55.3991	15.8099	55.7683	16.76276	55.3242	16.20458	55.0611
63	15.3155	55.3918	15.92313	55.8023	17.01789	55.2995	16.44627	55.0899
64	15.61966	55.3792	16.4028	55.8827	17.15846	55.2928	16.46594	55.1017
65	15.62688	55.3801	16.45386	55.8901	17.49878	55.2561	16.79735	55.2306
66	16.18709	55.4144	16.54692	55.9036	17.761	55.2075	17.02291	55.3104
67	16.34716	55.432	16.89059	55.9827	18.0594	55.1349	17.71802	55.4014
68	16.45761	55.4307	17.01977	56.0254	18.34781	55.0686	17.98295	55.4376
69	16.83807	55.4522	17.36337	56.1084	18.4412	55.0393	17.99429	55.4442
70	17.13592	55.4959	17.7341	56.1932	18.84665	54.9217	18.09436	55.5357
71	17.29731	55.5087	17.87861	56.2278	19.07773	54.8618	18.21232	55.6053
72	17.53084	55.5203	18.04312	56.2842	19.19438	54.8295	18.88456	56.0186
73	17.98631	55.6352	18.3932	56.3939	19.39554	54.778	18.98819	56.0942
74	17.99722	55.6377	18.71565	56.5651	19.66851	54.6963	19.06226	56.1592
75	18.00473	55.6389	18.90574	56.7287	19.79802	54.6574	19.50442	56.3947
76	18.30644	55.7153	19.10337	56.9759	19.88772	54.6249	19.54407	56.4212
77	18.55564	55.7444	19.38826	57.0823	20.11582	54.5533	19.9879	57.8707
78	18.6735	55.7606	19.52815	57.4374	20.289	54.4886	20.04999	58.1173
79	18.80582	55.7838	19.92716	58.4897	20.70993	54.4438	20.56327	60.5141
80	19.29722	55.8655	20.10966	58.7498	20.95926	54.407	20.58989	60.5875
81	19.38892	55.8785	20.389	58.8943	21.55351	54.3883	20.68323	60.66
82	19.66018	55.9102	20.63006	59.031	21.56169	54.3892	21.12219	60.9927
83	19.96596	55.9213	20.88154	59.1193	21.79108	54.4322	21.2864	61.0299
84	20.22643	55.9263	21.29492	59.2381	22.24556	54.4425	21.65244	61.1789
85	20.44984	55.9379	21.55953	59.4524	22.43143	54.463	21.7068	61.2158
86	20.7409	55.9659	21.71	59.4619	22.81365	54.595	21.85312	61.1932
87	20.74218	55.9661	21.92582	59.5937	22.88849	54.6265	23.76582	61.1315
88	20.7474	55.9664	22.03797	59.5903	23.9697	58.1495		
89	21.4365	56.0433	22.12398	59.6219	24.10591	58.565		
90	21.48309	56.0778	22.4378	59.8052	24.23234	58.5943		
91	21.9519	56.7593	22.65009	59.9371	24.48262	58.6453		
92	22.10253	56.9631	23.17912	59.9493	24.64617	58.6709		
93	22.12399	57.013	23.42028	60.306	24.98868	58.7065		
94	22.47305	57.6555	23.54241	60.2927	25.39658	58.6992		

95	22.90628	59.2504	23.65008	60.2897	25.44768	58.6977
96	22.92773	59.3393	23.94346	60.6729	25.5869	58.7234
97	22.94017	59.3473	24.4267	60.6177	25.71155	58.7465
98	23.91214	60.5943	25.79109	60.9148	25.92695	58.788
99	24.01065	60.6553	25.92165	60.8093	26.46457	58.9283
100	24.05562	60.6818	26.04323	60.6191	26.47599	58.9324
101	24.28997	60.7692	26.16189	60.5461	26.48139	58.9343
102	24.91332	61.0481	26.45702	60.5592	26.59375	58.9716
103	25.0725	61.1376	27.01	60.1409	27.22922	59.1831
104	25.24745	61.0635	27.21219	60.2597	27.32019	59.2266
105	30.725	61.0396	27.38357	60.193	27.75424	59.4896
106			27.74765	60.2923	28.07992	59.6463
107			28.24626	60.4627	28.18555	59.7196
108			28.80928	60.6233	28.29726	59.781
109			29.10569	60.6274	28.46036	59.9374
110			29.25751	60.7108	28.79953	60.2402
111			29.3964	60.7779	29.03097	60.5062
112			29.48744	61.1906	29.21499	60.7515
113			33.09265	61.196	29.25984	60.8117
114			34.81577	61.0743	29.2883	60.8284
115					29.37433	60.8066
116					29.37624	60.8064
117					29.46106	60.5284
118					29.70492	61.2578
119					29.71655	61.2616